A drop in mid-summer shortwave radiation induced by changes in the ice-surface condition in the central Arctic

Jun Inoue,[1] Takashi Kikuchi,[1] Donald K. Perovich,[2] and James H. Morison[3]

Received 7 April 2005; revised 18 May 2005; accepted 2 June 2005; published 7 July 2005.

[1] Ice-surface changes during summer and effects on solar heat input in the Arctic were analyzed using incoming shortwave radiation data from drifting buoys deployed in 2002, 2003, and 2004 as part of the North Pole Environmental Observatory project. Observed shortwave radiation was about half of the incoming shortwave radiation at the top of the atmosphere during early summer, suggesting cloudy skies. In each year, events occurred after mid-summer during which time the shortwave radiation decreased 33% to one third of shortwave radiation at the top of the atmosphere. Snow-depth data, aerial photos, and date of melt onset at the buoy site suggest that a decrease in snow/ice albedo induced by snow melting and melt-pond formation modified the amount of shortwave radiation through multiple reflections. A simplified calculation of the ice-albedo feedback revealed that the drop in shortwave radiation after mid-summer was self damping. **Citation:** Inoue, J., T. Kikuchi, D. K. Perovich, and J. H. Morison (2005), A drop in mid-summer shortwave radiation induced by changes in the ice-surface condition in the central Arctic, *Geophys. Res. Lett.*, *32*, L13603, doi:10.1029/2005GL023170.

1. Introduction

[2] The interaction between sea ice and heat input into the ocean through the ice-albedo feedback mechanism is one of the most important processes driving the Arctic climate [e.g., *Curry et al.*, 1995]. A key parameter controlling ice-albedo feedback is the seasonal evolution of surface albedo. As *Shine* [1984] pointed out, areas with high albedo have multiple reflections between the atmosphere (particularly clouds) and the snow/ice surface that force a different radiative flux than areas with low albedo. The effect of high surface albedo on incoming shortwave (SW) radiation was first reported by *Nansen* [1897], who used the 'dark' underside of stratus clouds to navigate to open water. *Wendler et al.* [2004] found that incoming radiation under overcast conditions in Antarctica was 85% higher for a highly reflective surface than for a water surface because of multiple reflections. In addition, changes in the summer snow/ice albedo in the Arctic strongly influence surface melt-pond hydrology [e.g., *Grenfell and Perovich*, 2004; *Eicken et al.*, 2004]. Albedo of ponded ice typically ranges from 0.2 to 0.4 [*Perovich et al.*, 2002]; the aerial surface albedo is strongly modified in areas with consistent ice cover.

[3] Shortwave radiation penetrating into open water can become a dominant heat source to warm surface ocean waters and subsequently melt the lateral and bottom of adjacent sea ice [*Maykut and Perovich*, 1987; *Maykut and McPhee*, 1995]. Data from a drifting buoy [*McPhee et al.*, 2003] showed that storage and release of SW radiation energy in the ocean boundary layer during summer dominated heat flux below the Arctic sea ice. A rapid increase in melt rate in late summer is linked to a buildup of heat in the water plus a sharp jump in floe speed [*Perovich et al.*, 2003].

[4] The North Pole Environmental Observatory (NPEO) was designed in 2000 to track and describe ongoing changes in the Arctic environment, and to provide long-term data and infrastructure resources for other polar science and climate investigations. The NPEO includes automated drifting buoy stations fixed to the sea ice, an ocean mooring, and airborne hydrographic surveys [*Morison et al.*, 2002]. Recent oceanographic results have focused on the heat flux under the Arctic sea ice [*McPhee et al.*, 2003] and the evolution of the cold halocline [*Kikuchi et al.*, 2004]. To understand the coupled atmosphere-ice-ocean system, however, the impact on the SW radiation of any change in ice-surface conditions must be investigated.

2. Observations

[5] Observations considered in the present study were gathered from radiometer and mass balance buoys and a meteorological station installed by NOAA's Pacific Marine Environmental Laboratory (PMEL) and the US Army's Cold Regions Research and Engineering Laboratory (CRREL). The NPEO buoy cluster was deployed on 29 April 2002 (at 88.5°N, 71.6°E), 29 April 2003 (at 88.9°N, 76.2°E), and 28 April 2004 (at 89.3°N, 117.3°E) and subsequently drifted slowly southward (Figure 1). By the end of March, the buoy cluster was exiting the Arctic through the Fram Strait. This study uses data from May to September in each NPEO year to investigate changes in SW radiation over central Arctic ice. In addition to the buoy data, ice concentration derived from the Special Sensor Microwave Imager (SSM/I), and North Pole Web-cam images from NOAA/PMEL were utilized for this study.

[6] Global solar radiation was observed by a Kipp & Zonen CM22 Pyranometer installed on a radiometer buoy. The pyranometer measures downward SW radiation at wavelengths between 305 and 3600 nm with an directional error of ±5 Wm^{-2}. A heater and a fan constantly blew air over the radiometer surface. Because the heater and fan were powered by solar panels, data were not available after

[1]Institute of Observational Research for Global Change, Independent Administrative Institution, Japan Agency for Marine-Earth Science Technology (JAMSTEC), Yokosuka, Japan.
[2]Engineer Research and Development Center, Cold Regions Research and Engineering Laboratory, Hanover, New Hampshire, USA.
[3]Polar Science Center, Applied Physics Laboratory, University of Washington, Seattle, Washington, USA.

0094-8276/05/2005GL023170$05.00

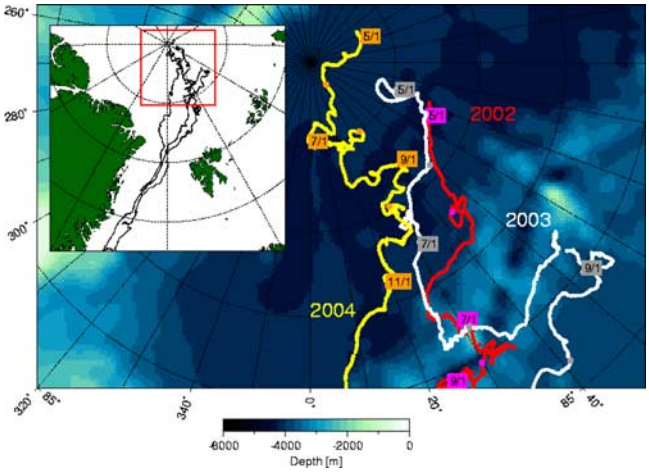

Figure 1. Drifting trajectory of 2002 (red), 2003 (white), and 2004 (yellow).

mid- to late September when the heater and fan ceased functioning. The mass balance buoy carries an acoustic pinger that measures snow depth on top of the sea ice. It also carries a chain of thermistors that measure temperatures from the air down through the snow cover, through the sea ice, and into the seawater below. The chain is several meters long and has temperature sensors every 5–10 cm. The meteorological station measures wind speed and direction, and air temperature and pressure. A North Pole Web-cam was deployed in each NPEO year. Images from the camera documented North Pole snow cover, weather conditions, and NPEO instrumentation status. All buoys were near each other on the same floe, and all data were transmitted by the NOAA Argos satellite.

[7] Meteorological observations vary among the NPEO years. Air temperatures averaged between May and September in 2002 were the coldest of the three years (−4.5°C in 2002, and −3.6°C in 2003 and 2004), so melt onset was delayed in 2002 as discussed in the next section. The summer of 2004 was characterized by relatively weak wind speeds (10.2 m s^{-1} in 2002, 9.9 m s^{-1} in 2003, and 7.5 m s^{-1} in 2004); therefore the floe drift distance between May and September was shortest in this year (Figure 1). Variability in the meteorology must be considered when discussing how changes in the ice-surface condition affect SW radiation.

3. Results

[8] Figure 2 shows a time series of observed SW radiation (ten-day mean value; black line). For reference, SW radiation at the top of atmosphere at the exact buoy location was calculated (hereafter SW_{TOA}; gray line) using a radiative transfer model [*Key*, 2001]; $SW_{TOA}/2$ (red line) and $SW_{TOA}/3$ (blue line) are also superimposed on Figure 2. From early summer until mid-June, the observed SW radiation is about half of SW_{TOA} regardless of the buoy position, which varies from year to year. Shortwave radiation amounts reflect the persistence of clouds in the Arctic summer [e.g., *Intrieri et al.*, 2002; *Inoue et al.*, 2005]. Observed SW radiation dropped from $SW_{TOA}/2$ to $SW_{TOA}/3$, a 33% reduction, after mid-summer. The exact timing of the drop, henceforth the 'SW-drop event', varied for each year, and the events ended within about two weeks.

[9] Snow depth decreased from mid-July to mid-August before the SW-drop event as air temperatures approached zero (see Figure 3) for 2002. Surface conditions changed

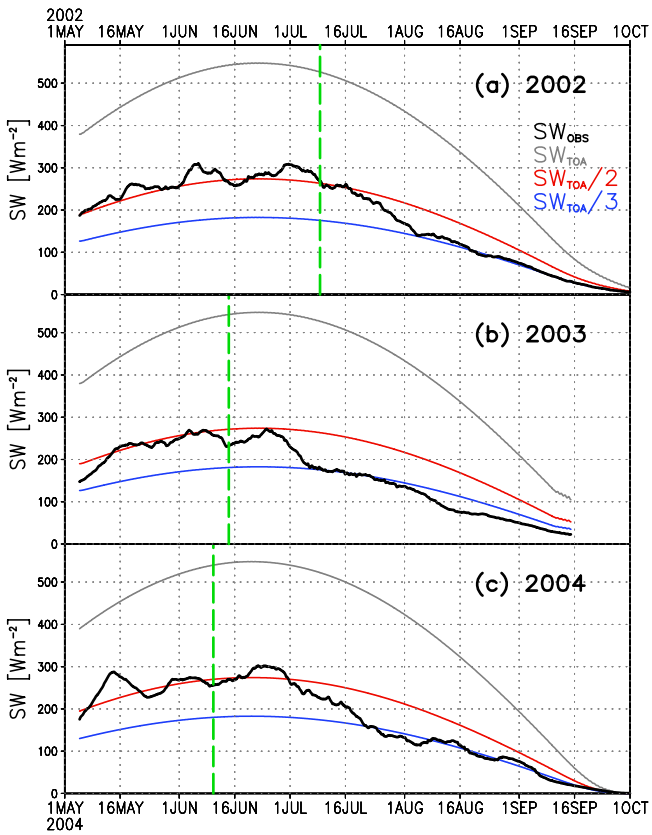

Figure 2. Ten-day average global radiation at the top of the atmosphere (SW_{TOA}: gray), $SW_{TOA}/2$ (red), $SW_{TOA}/3$ (blue), and observed values (black) for (a) 2002, (b) 2003, and (c) 2004. Melt onset is indicated by a green dashed line.

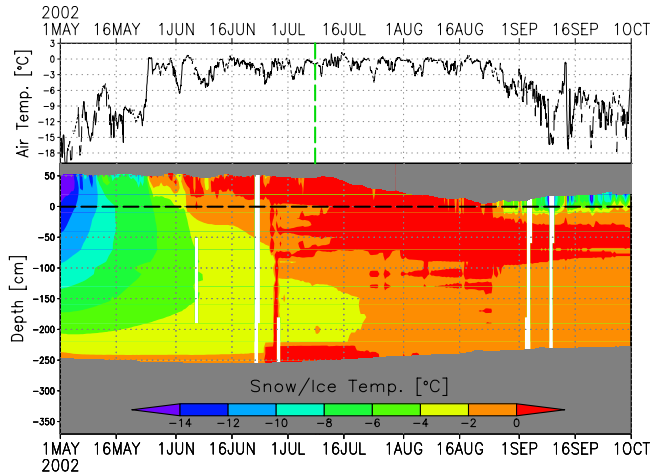

Figure 3. Air temperature (top) and temperatures from the ice surface down through the ice (bottom) from the 2002 deployment. Melt onset is indicated by a green dashed line. The black dashed line denotes the boundary between snow and ice.

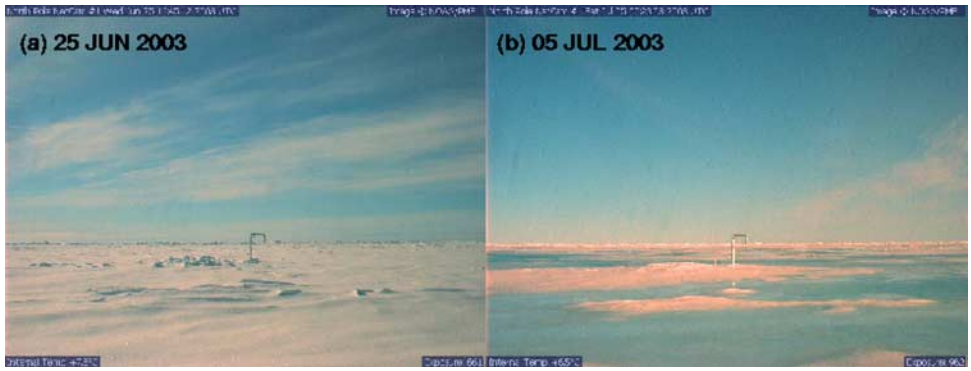

Figure 4. Web-cam images on (a) 25 June 2003 and (b) 5 July 2003. A mass balance buoy is at the center of the image.

from snow-covered ice to bare ice with melt ponds, and the surface albedo decreased significantly. As the surface albedo decreased, it is considered that incoming SW radiation decreased steadily through multiple reflections because relatively more SW radiation was absorbed at the surface. *Shupe and Intrieri* [2004] showed that a reduction of 0.1 in the surface albedo decreased incoming SW radiation by about 40 W m^{-2} for typical late-spring Arctic conditions. This is a negative radiative feedback. The difference between $SW_{TOA}/2$ and $SW_{TOA}/3$ during mid-summer in NPEO years is about 100 W m^{-2}, suggesting that an aerial albedo change during the SW-drop event is roughly estimated 0.25. The decrease in the aerial albedo does not arise from a decrease in ice cover; ice concentration near the North Pole remained about 95% and does not change rapidly. The decrease in aerial albedo is attributed mainly to snow melt and the formation of melt ponds.

[10] Melting usually begins in mid-June poleward of 80°N [e.g., *Rigor et al.*, 2000; *Belchansky et al.*, 2004]. The exact date of melt onset for each NPEO year was estimated using criteria from *Rigor et al.* [2000] (i.e., a 14-day running mean of the 2-m temperature and a −1°C threshold for the melt season). Estimated dates are 9 July 2002, 15 June 2003, and 11 June 2004 (green dashed line in Figure 2). Melt onset in 2002 is about three weeks later than normal, reflecting the colder mean air temperature during 2002. The SW-drop event started about two weeks after melt onset in each year. The SW-drop event in 2003 ended within 10 days (between 25 June and 5 July 2003). Web-cam images on 25 June and 5 July (Figure 4) clearly show the abrupt evolution of melt ponds. Pond fraction is estimated at 30–40% from the image. These observations also support the idea that changes in the surface condition influence multiple reflections and therefore the incoming SW radiation.

4. Discussion

[11] The SW-drop event damps the ice-albedo feedback mechanism after mid-summer, because lateral melting is reduced. The amount of heat supplied to a unit area of the upper ocean system (F_o) can be approximated by the SW radiation at the water surface (F_{sw}) and ice concentration (A_i), i.e., $F_o \propto F_{sw} \times (1 - A_i)$. The SW-drop amount in this study can therefore be related to an apparent increase of ice concentration. For example, a 33% reduction in the SW radiation is equivalent to a 0.33% increase in ice concentration for 99% ice concentration or an apparent increase of 0.99% and 1.65% for 97% and 95% ice concentrations, respectively.

[12] The evolution of ice concentration from spring to fall in 2002 in the central Arctic was calculated to determine the effect of the SW-drop event on the ice-albedo feedback. The simplest case was assumed: all solar energy absorbed is immediately and completely used in lateral melting, and any change in ice thickness is negligible. For such a case, the following simple relationship is satisfied,

$$F_o = A_w(1 - \alpha)F_{sw} = \rho_i L_f H \frac{dA_w}{dt} \quad (1)$$

where A_w is the area of open water (= $1 - A_i$), $\alpha = 0.1$ is the albedo of water, $\rho_i = 900$ kg m^{-3} is the density of ice, $L_f = 0.335$ M J kg^{-1} is the latent heat of fusion of ice, $H = 2.5$ m is the ice thickness (Figure 3), and t is time. The area of open water at initial time $t = 0$ is $A_w = 1$, 2, 3, 4, and 5%, corresponding to ice concentrations of $A_i = 99$, 98, 97, 96, and 95%, respectively. The daily mean SW radiation at the surface at the buoy position for the 2002 deployment

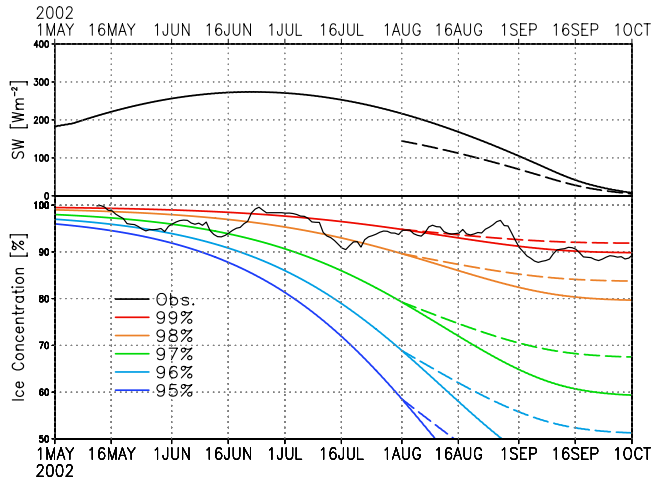

Figure 5. SW radiation used to calculate the ice-albedo feedback for $SW_{TOA}/2$ (solid line) and $SW_{TOA}/3$ (dashed line) (top), and the evolution of ice concentration calculated from the different initial ice concentration (bottom). Ice concentration observed by SSM/I at the nearest buoy position is indicated by the solid line.

was half the value of daily mean SW_{TOA} (Figure 2a). After 1 August 2002, daily mean SW radiation decreased from $SW_{TOA}/2$ to $SW_{TOA}/3$ for the realistic case. Sensitivity of the SW-drop after mid-summer was tested by fixing the flux to $SW_{TOA}/2$ (Figure 5, top).

[13] Figure 5 (bottom) shows the time evolution of ice concentration under different initial conditions. Although differences in initial ice concentration can be very small, the amount of open water area is very different. Consequently, the differences in A_w at the end of September are amplified; for example, A_w on 1 October was 8 times the initial state of $A_w = 1\%$ (i.e., $A_i = 99\%$; red line), but 11 times as large for the case of $A_w = 3\%$ (i.e., $A_i = 97\%$; green line). The evolution of observed ice concentration, an area-averaged value derived from SSM/I (75×75 km^2), agrees with the $A_i = 99\%$ calculation, suggesting that an ice-albedo feedback occurs even in areas that are primarily ice-covered. The impact of the SW-drop event on the ice-albedo feedback is strongest when initial ice concentration is small; differences between $SW_{TOA}/2$ and $SW_{TOA}/3$ cases on 1 October are 2% when $A_i = 99\%$ (red line) and 8% when $A_i = 97\%$ (green line). The ice-albedo feedback in areas of low ice concentration is sensitive to the SW-drop event.

[14] In simulations, sea-ice will decay quickly unless the SW-drop event is accurately reproduced: surface albedos, snow cover, and pond fraction must be well simulated. However, climate models use a wide variety of parameterizations for snow/ice albedos. Therefore, the seasonal cycle of albedo differs significantly from observations (see *Curry et al.* [2001] for a review). As part of the Arctic Regional Climate Model Intercomparison Project (ARCMIP) [*Curry and Lynch*, 2002], Liu et al. (personal communication, 2005) reported that more complex snow/ice albedo treatments (i.e., functional relationships of snow depth, ice thickness, and surface temperature) yielded more realistic ice cover and thickness distributions. A more sophisticated snow/ice albedo treatment is indispensable for better modeling and understanding of precise ice-albedo feedback mechanisms and radiative exchanges in the coupled atmosphere-ice-ocean system.

[15] **Acknowledgments.** We are sincerely grateful to all participants in the NPEO buoy deployments. We thank James E. Overland and Jacqueline A. Richter-Menge for providing us with buoy data. Discussions with Sohey Nihashi were helpful. Project support is provided by JAMSTEC and the following NSF Grants: OPP-9910305 and OPP-0352754.

References

Belchansky, G. I., D. D. Douglas, and N. G. Platonov (2004), Duration of the Arctic sea ice melt season: Regional and interannual variability, 1979–2001, *J. Clim.*, *17*, 67–80.

Curry, J. A., and A. H. Lynch (2002), Comparing Arctic regional climate models, *Eos Trans. AGU*, *83*(9), 87.

Curry, J. A., J. L. Schramm, and E. E. Ebert (1995), Sea ice-albedo climate feedback mechanism, *J. Clim.*, *8*, 240–247.

Curry, J. A., J. L. Schramm, D. K. Perovich, and J. O. Pinto (2001), Applications of SHEBA/FIRE data to evaluation of snow/ice albedo parameterizations, *J. Geophys. Res.*, *106*, 15,345–15,355.

Eicken, H., T. C. Grenfell, D. K. Perovich, J. A. Richter-Menge, and K. Frey (2004), Hydraulic controls of summer Arctic pack ice albedo, *J. Geophys. Res.*, *109*, C08007, doi:10.1029/2003JC001989.

Grenfell, T. C., and D. K. Perovich (2004), Seasonal and spatial evolution of albedo in a snow-ice-land-ocean environment, *J. Geophys. Res.*, *109*, C01001, doi:10.1029/2003JC001866.

Inoue, J., B. Kosović, and J. A. Curry (2005), Evolution of a storm-driven cloudy boundary layer in the Arctic, *Boundary-Layer Meteorol.*, in press.

Intrieri, J. M., M. D. Shupe, T. Uttal, and B. J. McCarty (2002), An annual cycle of Arctic cloud characteristics observed by radar and lidar at SHEBA, *J. Geophys. Res.*, *107*(C10), 8030, doi:10.1029/2000JC000423.

Key, J. (2001), *Streamer User's Guide*, 99 pp., Coop. Inst. for Meteorol. Satell. Stud., Univ. of Wis., Madison.

Kikuchi, T., K. Hatakeyama, and J. H. Morison (2004), Distribution of convective lower halocline water in the eastern Arctic Ocean, *J. Geophys. Res.*, *109*, C12030, doi:10.1029/2003JC002223.

Maykut, G. A., and D. K. Perovich (1987), The role of shortwave radiation in the summer decay of a sea ice cover, *J. Geophys. Res.*, *92*, 7032–7044.

Maykut, G. A., and G. M. McPhee (1995), Solar heating of the Arctic mixed layer, *J. Geophys. Res.*, *100*, 24,691–24,703.

McPhee, G. M., T. Kikuchi, J. H. Morison, and T. P. Stanton (2003), Ocean-to-ice heat flux at the North Pole Environmental Observatory, *Geophys. Res. Lett.*, *30*(24), 2274, doi:10.1029/2003GL018580.

Morison, J. H., et al. (2002), North Pole Environmental Observatory delivers early results, *Eos Trans. AGU*, *83*(33), 357, 360–361.

Nansen, F. (1897), In Nacht und Eis, in *Die Norwegische Polar-Expedition, 1893–1896*, vol. 1, Brockhaus, Leipzig, Germany.

Perovich, D. K., W. B. Tucker III, and K. A. Ligett (2002), Aerial observations of the evolution of ice surface conditions during summer, *J. Geophys. Res.*, *107*(C10), 8048, doi:10.1029/2000JC000449.

Perovich, D. K., T. C. Grenfell, J. A. Richter-Menge, B. Light, W. B. Tucker III, and H. Eicken (2003), Thin and thinner: Sea ice mass balance measurements during SHEBA, *J. Geophys. Res.*, *108*(C3), 8050, doi:10.1029/2001JC001079.

Rigor, I. G., G. L. Colony, and S. Martine (2000), Variations in surface air temperature observations in the Arctic, 1979–97, *J. Clim.*, *13*, 896–914.

Shine, K. P. (1984), Shortwave flux over high albedo surfaces, *Q. J. R. Meteorol. Soc.*, *110*, 747–764.

Shupe, M. D., and J. M. Intrieri (2004), Cloud radiative forcing of the Arctic surface: The influence of cloud properties, surface albedo, and solar zenith angle, *J. Clim.*, *17*, 616–629.

Wendler, G., B. Moore, B. Hartmann, M. Stuefer, and R. Flint (2004), Effects of multiple reflection and albedo on the net radiation in the pack ice zones of Antarctica, *J. Geophys. Res.*, *109*, D06113, doi:10.1029/2003JD003927.

J. Inoue and T. Kikuchi, Institute of Observational Research for Global Change, Independent Administrative Institution, Japan Agency for Marine-Earth Science Technology (JAMSTEC), Yokosuka, 237-0061, Japan. (jun.inoue@jamstec.go.jp)

J. H. Morison, Polar Science Center, Applied Physics Laboratory, University of Washington, Seattle, WA 98105-6698, USA.

D. K. Perovich, Engineer Research and Development Center, Cold Regions Research and Engineering Laboratory, 72 Lyme Road Hanover, NH 03755, USA.